(9)

OFFICE OF NAVAL RESEARCH

FINAL TECHNICAL REPORT

for

1 October 1989 through 31 March, 1992

for

Contract N00014-90-J-1279

R&T No.

Fundamental Properties and Device Applications of Ge_xSi_{1-x}/Si Superlattices

Kang L. Wang

University of California, Los Angeles
405 Hilgard Avenue
Los Angeles, CA 90024

Contents

List of Figures

1 Abstract

The purpose of the research was to perform scientific study and experimentation on potential new Si based devices for future optical and electronic applications. The research areas included novel detectors, modulators, sources, new properties, and other quantum devices using Si molecular beam epitaxy (Si-MBE) based quantum wells and superlattices. With the support of ONR, we have made significant advances in the understanding of optical properties of intersubband transition of $Si_{1-x}Ge_x$/Si multiple quantum wells, and the fabrication of multiple quantum well infrared detectors operating in the 8-12 μm range. Large many-body effects have been observed in δ-doped Si and heavily doped SiGe/Si quantum well structures. We have also investigated the Stark effect of type II SiGe/Si quantum well structures for optical modulator application in 1-2 μm range. For potential realization of Si-based light sources we have continued the study of luminescence from monolayer superlattices and strained alloy layers. In the area of transport properties, we have calculated the effective mass and mobility of holes in strained SiGe layers as a function of Ge composition.

2 Introduction

The purpose of the research was to perform scientific study and experimentation on potential new Si based devices for future optical and electronic applications. The research areas included novel detectors, sources, new properties, and other quantum devices using Si molecular beam epitaxy (Si-MBE) based quantum wells and superlattices. With the support of ONR, we have made significant advances in the understanding of optical properties of intersubband transition of $Si_{1-x}Ge_x$/Si multiple quantum wells, and the fabrication of multiple quantum well infrared detectors operating in the 8-12 μm range. Large many-body effects have been observed in δ-doped Si and heavily doped SiGe/Si quantum well structures. We have also investigated the Stark effect of type II SiGe/Si quantum well structures for optical modulator application in 1-2 μm range. For potential realization of Si-based light sources we have continued the study of luminescence from monolayer superlattices and strained alloy layers. In the following we highlight the accomplishments made. Details may

be referenced to the publications resulting from the past three years efforts listed in section 2.8.

2.1 δ-doped Quantum Wells and Many-Body Effects

In the following, we will describe the important properties of δ- doped quantum wells [1] that we have discovered. The key point is to show that the many-body effects due to δ-doping can be used to tune the transition energy, independent of effective mass. The δ-doping in semiconductors can be viewed as an alternative way of achieving quantum well structures without heterojunctions. The potential profile associated with δ-doping closely resembles that of a parabolic quantum well, due to the finite width of the doped layer. The well thickness and the barrier height can be controlled by the thickness of the doped layer and the doping density. The potential profile and the energy level spectrum in the well is usually obtained by solving the Schrödinger and Poisson's equations self-consistently (Hartree approximation) [2]. For intersubband detector application in the 10 μm range, the population of carriers in such structures needs to be considerably larger (in order to get the required energy level separation) than typically used in heterojunction quantum wells. As a result, the many-body effects play an important role in determining the optical properties of δ-doped quantum wells.

A typical structure used in this study consists of an undoped Si buffer layer, followed by 10 periods of 35 $\AA$ of heavily boron-doped Si layers and 300 $\AA$ of undoped Si spacers. Figure 1 shows the (SIMS) depth profile for a typical δ-doped structure (sample A). A full width at half maximum (FWHM) of approximately 50 Å is obtained from the depth profile.

Measured absorption spectra of samples with different doping densities as a function of photon energy are shown in Fig. 2. It can be clearly seen that the absorption spectra shift towards the high energy regime with increasing absorption as the doping density is increased. The shift of the absorption peak is mainly due to the increase of the potential well depth at high doping densities. The widths of the absorption peaks are more than an order of magnitude larger than those observed in GaAs/AlGaAs quantum well structures, typically about 10 meV. The polarization dependence of the

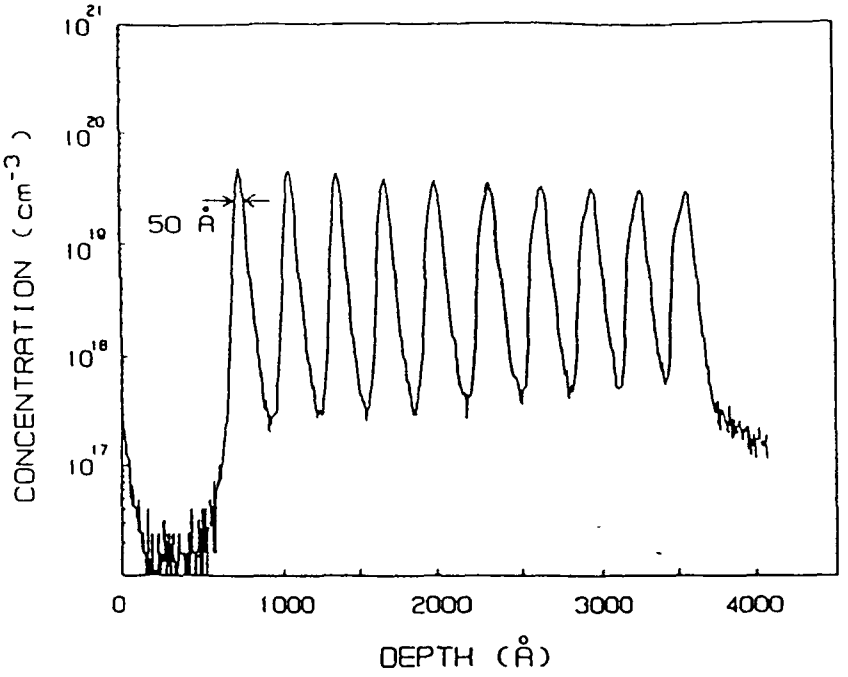

Figure 1: SIMS depth profile of sample A. It reveals 10 periods of boron δ-doped Si layers with a FWHM of about 50 Å.

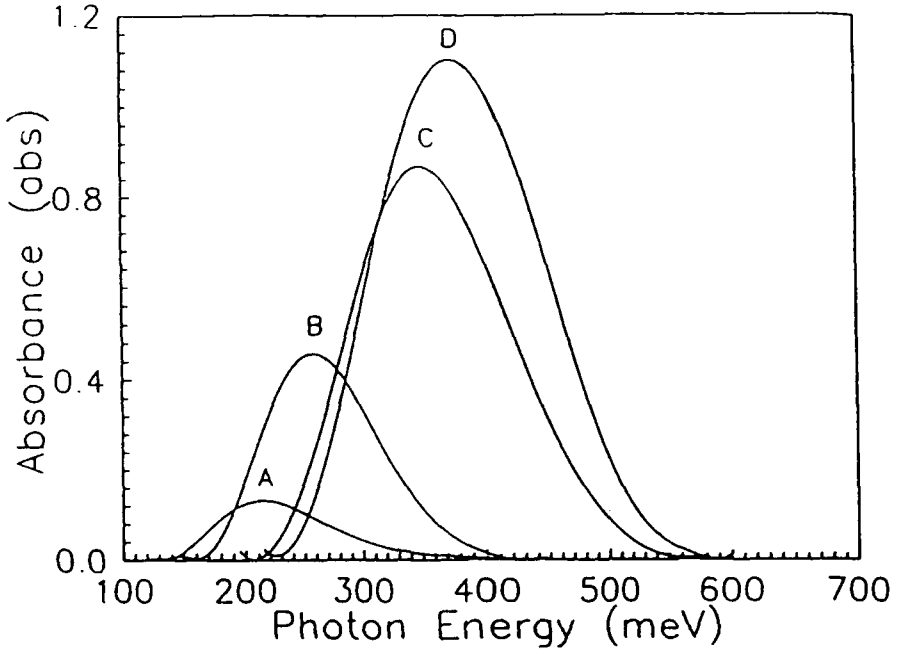

Figure 2: Absorption spectra of the four samples as a function of photon energy at 300 K. The set of curves is due to different doping concentrations.

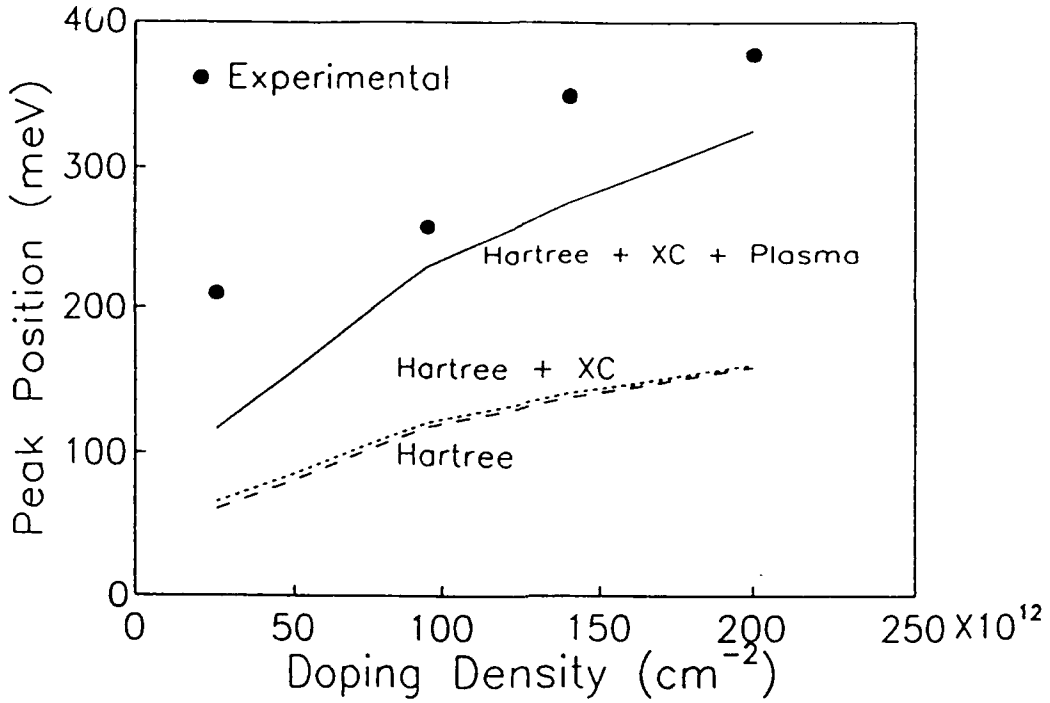

Figure 3: Subband separation as a function of doping density (a) experimental data (dashed curve with open circles), calculated results using (b) using the Hartree approximation (dashed curve), and (c) the Hartree-Fock approximation (solid curve).

spectra shows a similar behavior as in the case of multiple quantum wells discussed above, indicating the one dimensional nature of the potential.

The experimental peak positions along with the calculated values using a multiband self-consistent calculation (Hartree approximation) are shown in Fig. 3. These values are considerably smaller than the experimental values shown by the open circles. The solid curve in the Fig. 3 shows the incorporation of the many-body effects (i.e., Hartree-Fock approximation) to the calculated energy level separation. This brought the calculated and experimental peak positions to a reasonably close agreement. The significance of this work demonstrates the substantially large many-body effects of SiGe than those of the GaAs-based system.

2.2 Intersubband Absorption in SiGe/Si Quantum Wells

The following examples will demonstrate the work to date in the intersubband transition and ability to quantify the polarization dependence [3]. The work described below is for p-type (100) and the transition obtained is between two heavy hole subbands and thus has the same selection rule as the AlGaAs/GaAs conduction subband

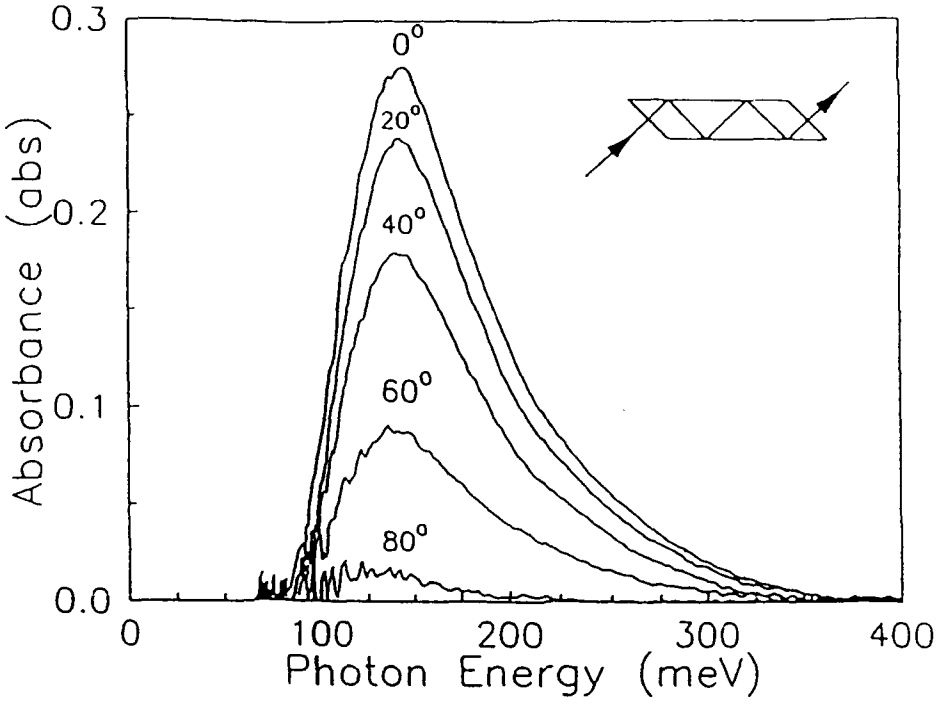

Figure 4: Measured absorption spectra as a function of energy for different polarization angles of the incident infrared beam. The absorption strength at large polarization angles is shown to decrease in accordance with the selection rules of intersubband transition at the Γ- point. The inset shows the waveguide structure used in the measurement.

transition. In the case of SiGe grown on Si, most of the band offset appears in the valence band and the intersubband absorption of holes can be more conveniently studied. The transmission spectrum of the sample is taken at room temperature using a Fourier transform infrared (FTIR) spectrometer. In the measurement, a waveguide structure of 5 mm long and 0.5 mm thick is employed (see inset of Fig. 4) in order to enhance the absorption.

Measured absorption spectra as a function of energy using the waveguide structure are shown in Fig. 4. The set of curves are due to different polarization angles of the infrared beam and the zero degree corresponds to the polarization of the beam along the growth direction. The strength of the intersubband absorption decreases as the polarization of the infrared beam is rotated from the perpendicular direction towards the parallel direction of the plane of layers. Figure 5 illustrates the relative absorption strength as a function of the polarizer angle ϕ and the data follow the $\cos^2\phi$ dependence (dashed curve), in good agreement with the selection rule of the intersubband transition. The estimated oscillator strength using the absorption data is about 0.98, which is in good agreement with the calculations. The value is also close

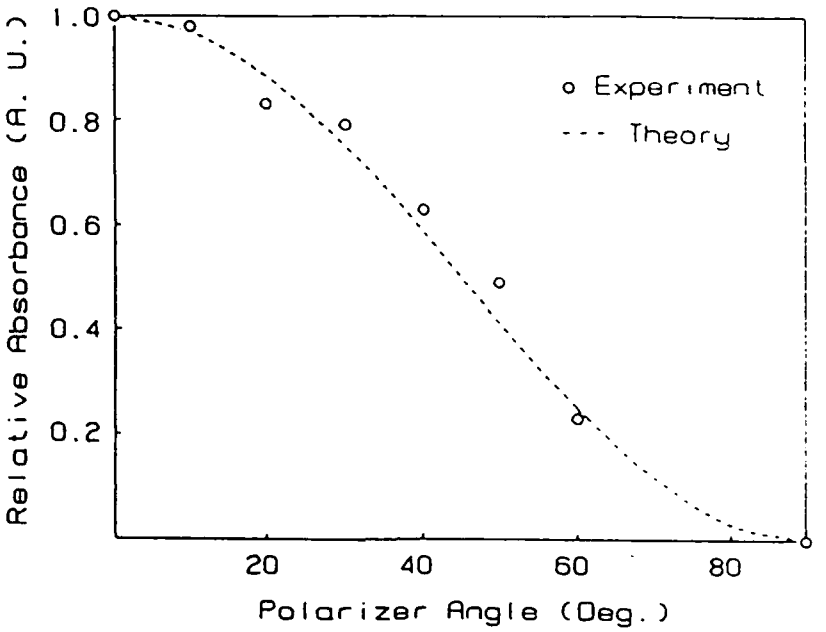

Figure 5: Normalized absorption strength as a function of the polarization of the incident infrared beam. The zero degree corresponds to the polarization along the growth direction of the structure. The dashed curve shows the theoretically expected $\cos^2\phi$ dependence.

to that obtained for intersubband absorption in III-V based quantum well structures which are in the 0.5 to 1.2 range.

2.3 Detector Application

We have investigated the potential application of SiGe/Si multiple quantum wells for infrared detectors [4, 5]. The use of Si-based quantum well structures has an added advantage due to the potential for integrating with Si signal processing electronics in a monolithic manner. The Ge composition and the well thickness are selected to have the heavy hole bound state inside the well and the first extended excited state close to the continuum of the barriers for detector application.

Figure 6 shows the room temperature absorption spectrum for different polarization angles as a function of wavelength using a 45° multipass waveguide structure with dimensions of 4 mm long and 0.5 mm wide. At the 0° polarization, the incoming photon electric field has components both along the growth direction (z-direction) and parallel with the growth plane (xy-plane). In this case, the absorption spectrum consists of a relatively broad peak at near 9 μm superimposed on a monotonically

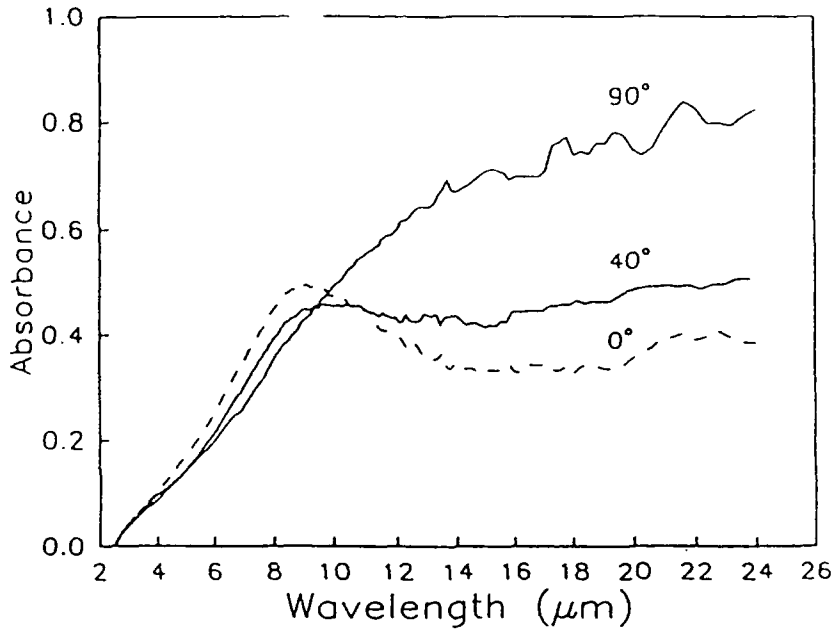

Figure 6: Measured FTIR spectrum at 300 K. Absorption spectra at three different polarization angles are shown. At the 0° polarization, a broad peak near 9 μm is seen. This peak is due to a heavy hole intersubband transition. The 90° case shows a stronger background absorption most likely due to free carrier absc- n, but the peak seen at the 0° polarization is not visible.

increasing background as the wavelength is increased. On the other hand at the 90° polarization where the field is polarized only along xy-plane, the absorption shows the similar trend as the 0° case, but the absorption strength is stronger and the peak at 9 μm is no longer visible. As the polarization angle increases, the peak absorption decreases (characteristics of intersubband transition at the Γ-point) while the background absorption increases. The absorption spectrum at the 90° polarization in Fig. 6 is mostly due to two dimensional free carrier absorption. In this case, the photon absorption occurs via phonon or impurity scattering to conserve the momentum. As the polarization angle increases, the photon field in xy-plane increases while the field in the z-direction decreases. This causes an increase of free carrier absorption and a decrease of intersubband absorption as the polarization angle increases.

Mesa diodes of 200 μm in diameter with a 45° facet on the edge of the wafer as shown in the inset of Fig. 7 are fabricated for the study of photoresponse. The infrared is illuminated on the facet at the normal such that the incident angle on the multiple quantum well structure is 45°. The photo-signals are measured at two different polarization angles of 0° and 90°. Figure 7 shows the photocurrents at

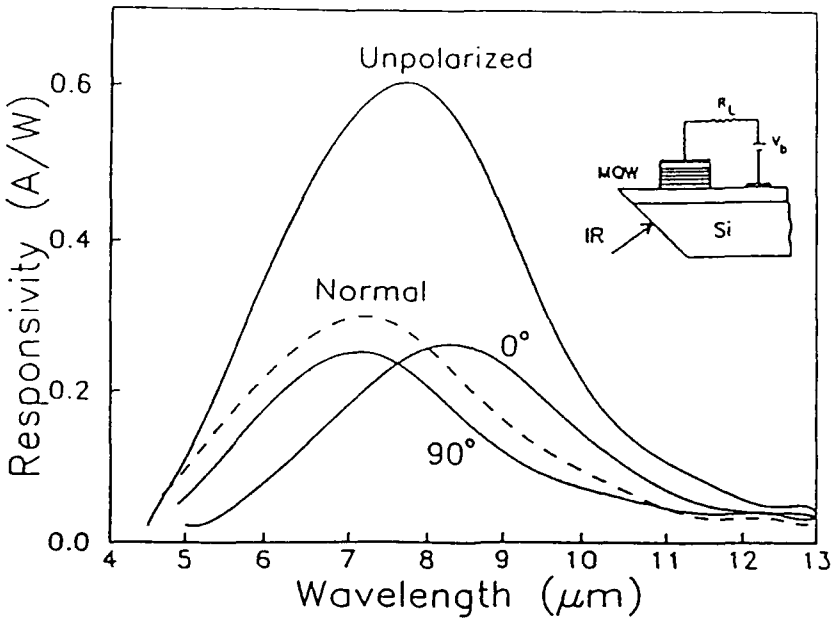

Figure 7: Photoresponse at 40 K for two polarizations angles with a 2 V bias applied across the detector. Infrared is illuminated on the facet at the normal such that the incident angle on the multiple quantum well structure is 45° as shown in the inset.

the 0° and 90° polarizations at 40 K, with a 2 V bias across the detector. In the 0° polarization case, a peak is found at near 8.6 μm which is in agreement with the FTIR absorption spectra, except the peak position moves slightly to a lower wavelength because of the use of different temperatures in the two measurements. The full width at half maximum (FWHM) is about 80 meV and is also in agreement with the absorption spectra, while for the 90° polarization, the peak at near 7.2 μm is observed with a similar FWHM. For the latter, the shift of the peak to a shorter wavelength may be due to the sharing of phonon energy with momentum conserving processes such as phonon or impurity scattering. The peak photocurrent found at the 0° polarization case disappears in this case. The photoresponse for both cases are about the same, 0.3 A/W. Fig. 7 shows the photocurrent along with the result obtained from a unpolarized beam. In the latter case, a peak is found at near 7.5 μm and the photocurrent is about 0.6 A/W, approximately the sum of two polarization cases.

It is clear that for the 0° polarization case, the photocurrent is due to intersubband transition between two heavy hole subbands and also partially due to internal photoemission of holes excited via free carrier absorption. For the 90° polarization case, intersubband transition is forbidden but free carrier absorption is stronger than that of the 0° polarization case because entire photon electric field lies in the xy-plane. The photocurrent in this case is believed to be due to internal photoemission of free carriers.

For the present not yet optimized detector, a quantum efficiency of $\eta \sim 14$ % is obtained for the polarized light. For the unpolarized case, the photocurrent is the sum of both intersubband transition and the photoemission due to free carriers.

2.4 Stark effect of type II SiGe/Si quantum wells

It is known that $Si_{1-x}Ge_x/Si$ heterostructures grown on a $Si_{1-y}Ge_y$ buffer layer has a type-II band (staggered) alignment where the quantum wells of electrons and holes are confined in different layers [6]. Due to the spatial separation of wave functions in the valence band (VB) and conduction band (CB), the structures with a type-II band alignment are expected to have optical properties different from those of type-I structures where both the CB and VB quantum wells are formed in the same layer. For example, in type-II multiple quantum well (MQW) structures, interband optical transition can have a large transition energy shift under an applied electric field. In the experiment, p-i-n diodes are fabricated in which the i-region consists of type-II SiGe/Si multiple quantum wells. The p-i-n diode structure consists of a p-doped (1×10^{18} cm^{-3}) $Si_{0.8}Ge_{0.2}$ unstrained buffer layer grown on a p-Si(100) substrate, 50 periods of undoped 70 Å $Si_{0.6}Ge_{0.4}$ quantum wells and 70 Å Si barriers, and a 0.8 μm n-doped (5×10^{16} cm^{-3}) $Si_{0.8}Ge_{0.2}$ cap layer terminated with a n^+ doped region for the ohmic contact [6].

The photocurrent measurement as a function of bias is carried out at 77 K in the wavelength range of 1-2 μm. Figure 8 shows the normalized photocurrent vs. photon energy as a function of applied reverse bias at 77 K. The measured photocurrent data have a strong bias dependence due to the increase of carrier transport under bias in the structure [6]. In order to deconvolute the spectral response from the carrier

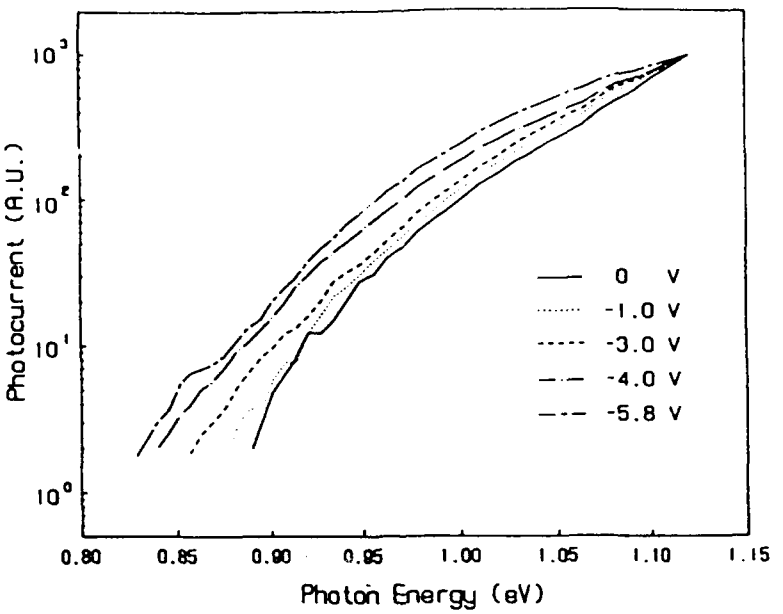

Figure 8: Normalized photocurrent spectra vs. photon energy (77 K) as a function of reverse bias across the p-i-n diode.

transport effect, the obtained photocurrent spectrum at each bias is normalized by the values at 1.1 eV for the same bias. As shown in Fig. 8, the absorption edges shift to lower energies (red shift) as the reverse bias across the p-i-n structure is increased. The amount of the shift is qualitatively given by the potential drop between the two spatially separated quantum wells, i.e., eEL/2, where E is the applied electric field and L is the period of MQW's. The experimental shifts are plotted as data points in Fig. 9. In the plot, the zero bias case is taken as the zero-field reference point. The dashed curve gives the calculated absorption energy shift versus electric field in the structure. An envelope function approximation is used for the calculation of the shift as a function of electric field [7]. For comparison, we have also included the calculated values for a type I MQW structure having parameters same as the type II structure. The measured slope of the shift as a function of electric field is approximately 0.75 meV/(kV cm^{-1}) and this value is close to the theoretically estimated value.

2.5 Optical Properties of Monolayer Si_mGe_n Superlattices

The optical properties of monolayer Si_mGe_n superlattices have been investigated by photoluminescence (PL) spectroscopy [8, 9]. The aim of this work is to understand

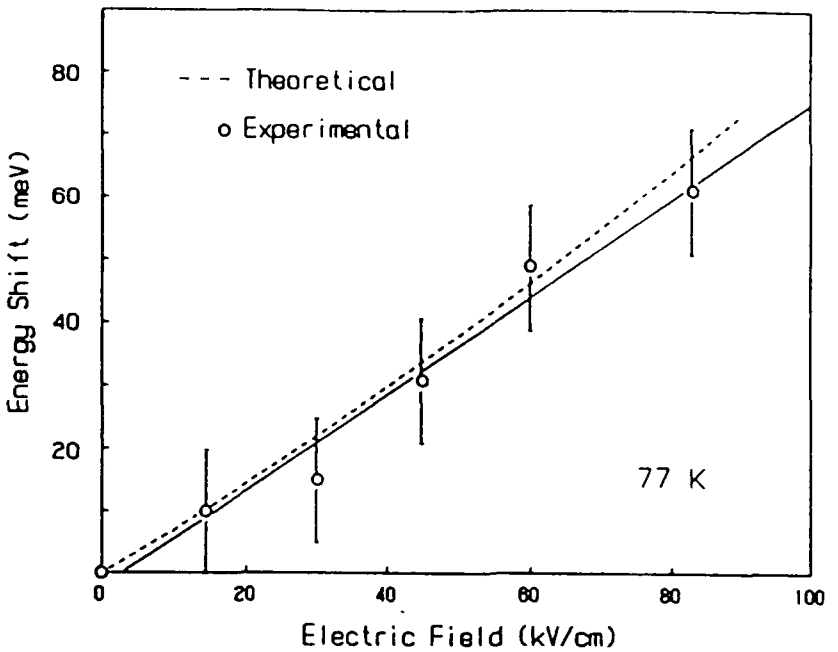

Figure 9: Electric field versus absorption edge shift at 77 K. The data points indicate the experimental values obtained using a curve fitting technique. The dashed curve shows the theoretical values. Note, zero bias is taken as the reference point.

the band-folding effects due to the short superlattice periodicity. In order to distinguish bandgap-related luminescence from defects and dislocations, the samples were passivated with atomic hydrogen. Fig. 10 shows the PL spectra, for example, of a 16×4 SL before and after passivation. The broad background luminescence in the low energy region is a characteristic of the D lines ascribed to dislocations in a plastically deformed SiGe buffer layer. Using a step by step chemical etching, the broad peak was shown to originate from the buffer layer. Upon passivation, this broad signal was considerably reduced in intensity and only two well defined peaks remained from the original spectrum. The 61 meV difference in energy between the two peaks was close to the Si-Si optical phonon vibration energy as measured by a Raman experiment. Thus the H-passivation study appears to confirm that the observed peaks at 1.026 eV and 0.965 eV are due to transitions in the SL. Similar behavior was also observed for the 14×4 superlattice with transitions at 0.998 eV and 0.940 eV. The lowering of the transition energy is due to the larger average Ge composition in the 14×4 superlattice compared with the 16×4 superlattice.

To further support the assertion that the 1.026 eV and 0.965 eV lines for the 16×4 SL (0.998 eV and 0.940 eV for the 12×4 SL) are superlattice-related, we have

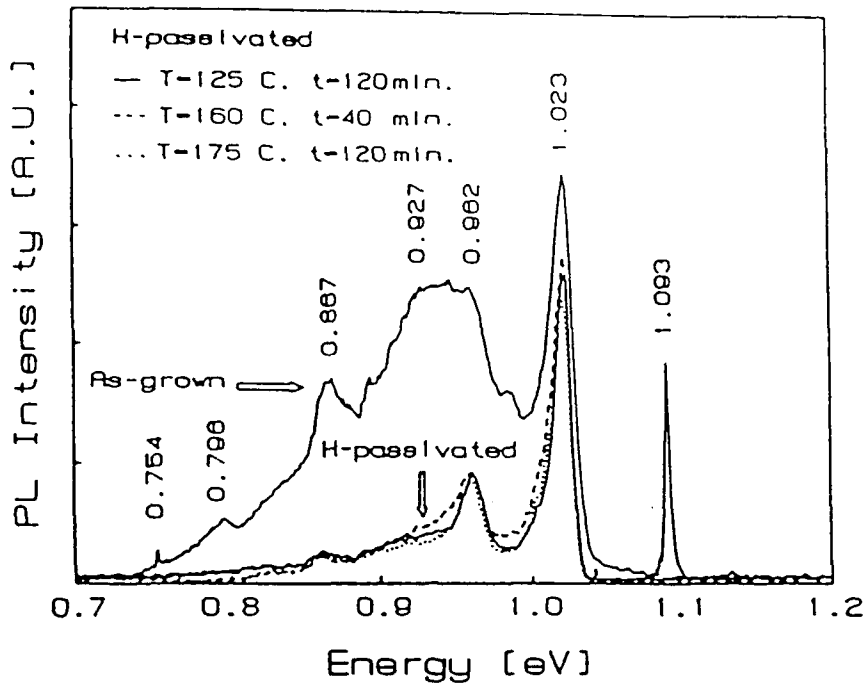

Figure 10: As-grown and hydrogenated photoluminescence spectra of a 16×4 superlattice. Hydrogenated spectra for three different temperatures and times are presented.

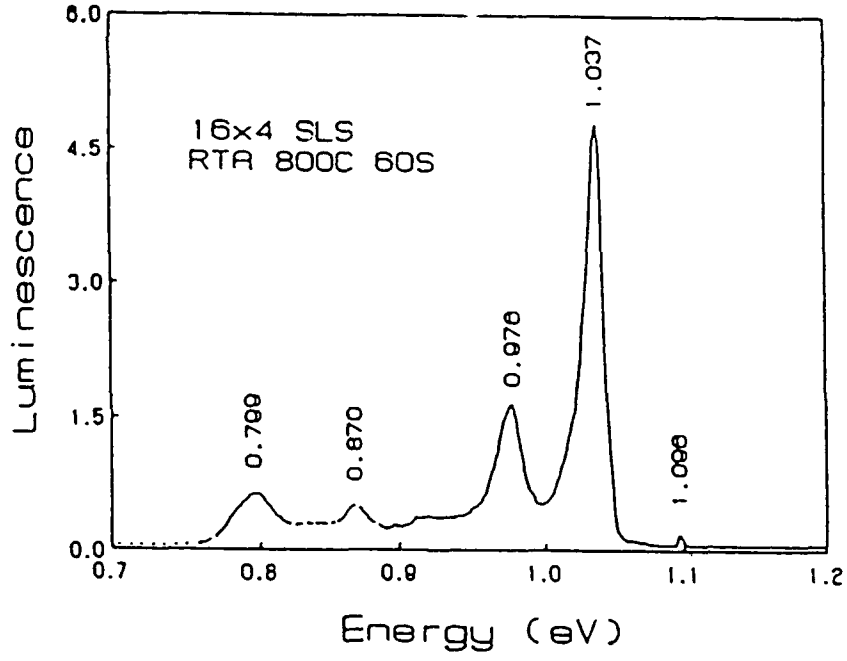

Figure 11: PL spectrum of the 16×4 SLS after an 800 °C, 60 second RTA. The peaks at 0.976 and 1.037 eV correspond, respectively, to the 0.965 eV shoulder and the 1.026 eV peak of the spectrum of the as-grown sample. The features at 0.799 and 0.870 eV are due to the buffer layer.

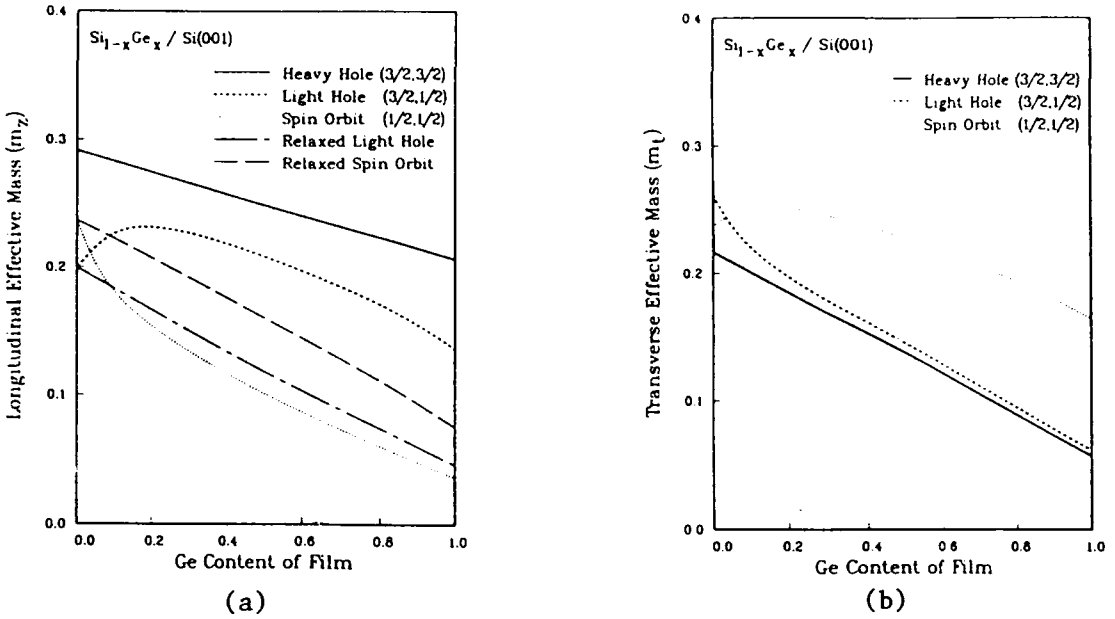

Figure 12: Calculated effective mass (a) longitudinal, and (b) traverse of strain SiGe layer grown on Si(100) substrate.

performed rapid thermal annealing (RTA) on the samples. The spectrum of the 16×4 SL after a RTA anneal at 800°C for 60 seconds is shown on Fig. 11 and is very similar to the spectrum obtained after hydrogenation. The two main peaks have shifted to higher energy due to the interdiffusion of the Si and Ge atoms at the interfaces. It is worth noting that the energy separation between the two peaks remains at 61 meV.

From these results, it is believed that the effect of the artificially introduced periodicity on the band structure is responsible for the observed superlattice PL signals, although no direct gap nature is confirmed. However, the observation of superlattice transition is a step towards better understanding of the light emission of zone-folded structures.

2.6 Effective mass and mobility of holes

The effective mass of the three hole bands of strained SiGe layers as a function of Ge composition have been calculated using the k·p and strain Hamiltonians. The constant energy surfaces of the valence bands under strain are shown to be ellipsoids for small k values and becomes similar to that of Si for large k values. The longitudinal and transverse effective masses for the three hole bands are shown in Fig. refmasses (a) and (b) for SiGe layers grown on Si (100) substrate. The transverse heavy hole

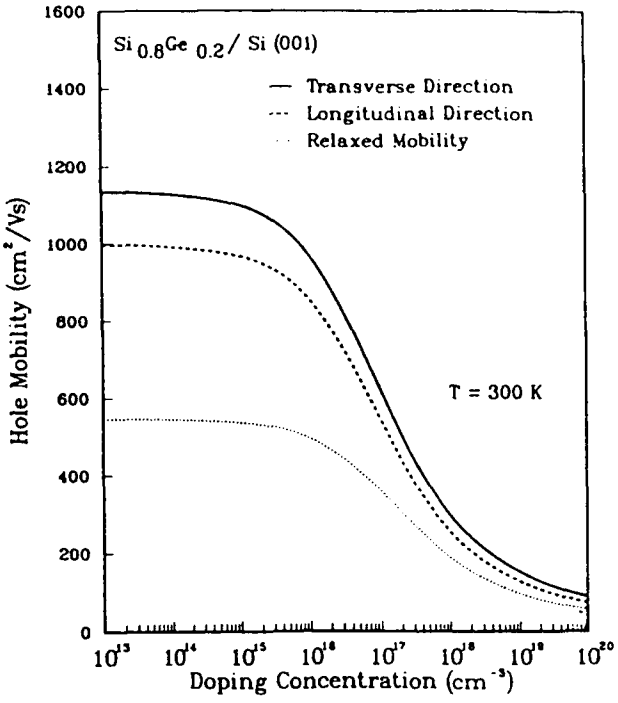

Figure 13: Calculate hole mobility of a strained $Si_{0.8}Ge_{0.2}$ layer as a function of temperature.

mass under strain becomes smaller than that of the light hole mass. On the other hand, the longitudinal heavy hole mass is unaffected by the strain [10]. We have also extended the calculation to estimate the hole mobility. Figure 13 shows the mobility of a $Si_{0.8}Ge_{0.2}$ layer grown on (100) oriented Si substrate as a function of temperature. We have shown that the phonon scattering is dominant in the high- temperature range and alloy scattering becomes important at low temperatures for $Si_{0.8}Ge_{0.2}$ film grown on (001) Si substrate. Under strain, the heavy and light hole degeneracy is lifted and thus reducing the interband scattering which gives higher mobility than that of relaxed layer of the same Ge composition. These results indicate the use of strain for further engineering of devices.

2.7 Summary

In summary, in the performance period we have studied the intersubband transitions in δ-doped quantum well structure in Si. The importance of many-body effects on the transition energy have been demonstrated for the first time. In the case of SiGe/Si heterostructures, intersubband transition between quantized states has been demonstrated for the first time. Infrared detectors operating near 10 μm have also been

fabricated. A large quantum confined Stark effect in a type-II SiGe/Si multiple quantum well structure have been demonstrated which can have potential application in optical modulators in the 1-2 μm range. As step towards achieving Si-based light sources, we have studied the luminescence of strained SiGe layers. The luminescence originated from the alloy was discriminated from those of dislocations using hydrogen passivation and progressively etching of the structure. In the study of transport properties, we have calculated the effective mass and mobility of strained SiGe layers as a function of Ge composition.

References

[1] J. S. Park, R. P. G. Karunasiri, and K. L. Wang. *Appl. Phys. Lett.*, 58, 1083, 1991.

[2] R. P. G. Karunasiri, J. S. Park, and K. L. Wang. *unpublished.*

[3] R. P. G. Karunasiri, J. S. Park and K. L. Wang. Long wavelength (10 μm) infrared detector using $si_{1-x}ge_x/si$ multiple quantum wells. In *DRC Proceeding*, 1991.

[4] R. P. G. Karunasiri, J. S. Park, and K. L. Wang. *Appl. Phys. Lett.*, 59, 2588, 1991.

[5] J. S. Park, R. P. G. Karunasiri, and K. L. Wang. *Appl. Phys. Lett.*, 60(1), 103, 1992.

[6] J. S. Park, R. P. G. Karunasiri, and K. L. Wang. *J. Vac. Sci. Technol.*, B8, 217, 1990.

[7] P. F. Yuh and K. L. Wang. *IEEE J. Quantum Electron.*, QE-25, 1671, 1989.

[8] M. A. Kallel, V. Arbet, R. P. G. Karunasiri, and K. L. Wang. *J. Vac. Sci. Tech.*, B8(2), 214, 1990.

[9] V. Arbet-Engels, M. A. Kallel, and K. L. Wang. *Appl. Phys. Lett.*, 59(14), 1705, 1991.

[10] S. K. Chun and K. L. Wang. *IEEE Trans. Electron Devices*, 39, 2153, 1992.

2.8 List of Publications

Manuscripts published or submitted

Rhee, S. S., Chang, G. K., Carns, T. K., and Wang, K. L., "SiGe Resonant Tunneling Hot Carrier Transistor", Proceedings IEEE/IEDM, 27.4.1, 651-654, (1989).

Park, J. S., Karunasiri, R. P. G., and Wang, K. L., "Observation of Large Stark Shift in Ge_xSi_{1-x}/Si Multiple Quantum Wells", J. Vac. Sci. Tech., B8, 217 (1990).

Mii, Y. J., Karunasiri, R. P. G., Wang, K. L., and Yuh, P. F., "Observation of Large Oscillator Strengths for Both 1- 2 and 1- 3 Intersubband Transitions of Step Quantum Well", Appl. Phys. Lett., 56, 1046 (1990).

Mii, Y. J., Karunasiri, R. P. G., Wang, K. L., Chen, M., and Yuh, P. F., "Large Stark Shifts of the Local to Global State Intersubband Transitions in Step Quantum Wells", Appl. Phys. Lett., 56, 1986 (1990).

Karunasiri, R. P. G., Park, J. S., Wang, K. L., and Chen, L- J., "Intersubband Infrared Absorption Ge_xSi_{1-x}/Si Superlattice by Photocurent Measurement", Appl. Phys. Lett., 56, 1342 (1990).

Karunasiri, R. P. G., Mii, Y. J., and Wang, K. L., "Tunable Infrared Modulator and Switch Using Stark Shifts in Step Quantum Wells", Electron Device Letters, 11, 227 (1990).

Rhee, S. S., Chang, G. K., Carns, T. K., and Wang, K. L., "SiGe Resonant Tunneling Hot Hole Carrier Transistor", Appl. Phys. Lett., 56, 1061 (1990).

V. Arbet, R. P. G. Karunasiri, and K. L. Wang, "PIN Photocurrent Studies of Monolayer Si_mGe_n Superlattices", SPIE 1286, (1990).

Karunasiri, R. P. G., Park, J. S., Mii, Y. J., and Wang, K. L., "Intersubband Absorption in $Si_{1-x}Ge_x$/Si Multiple Quantum Wells", Appl. Phys. Lett., 57, 2585 (1990).

Kallel, M. A., Arbet, V. P., Karunasiri, R. P. G., and Wang., K. L., "Photiluminescence Characterization of Si_mGe_n Superlattices", J. Vac. Sci. Technol. B8, 214 (1990).

Dafesh, P. A., Arbet, V. P., and Wang, K. L., ""Electronic Transitions in a Ge Rich-Symmetrized Si_mGe_n Strained Monolayer Measured by Photoreflectance Spectroscopy", Appl. Phys. 56, 1498 (1990).

Chang, S. J. , Arbet, V., Wang, K. L., Nayak, D. K., and Woo, J. C. S., "Studies of Inerdiffusion in Ge_mSi_n Strained Layer Superlattices ",J. Electronic Mat., 19, 125 (1990).

Prokes, S. M., Fatemi, and Wang, K. L., "X-ray Studies of Heat Treated Si/Ge Si Strained Layer Superlattice", J. Vac. Sci. Technol. B8, 254 (1990).

Glaser, E., Trombetta, J. M., Kennedy, T. A., Prokes, S. M., Glembocki, O. J., Wang, K. L., and Chern, C. H., "Detection of Magnetic Resonance on Photoluminescence from a Si/$Si_{1-x}Ge_x$ Strained- Layer Superlattices", Phys. Rev. Lett., 65, 1247 (1990).

Dafesh, P. A., Arbet, V. and Wang, K. L., "Electronic Transitions in a Ge Rich Strain-Symmetrized Si_8Ge_{32} Superlattice Measured by Photoreflectance Spectroscopy", SPIE 1286, 308 (1990).

Chang, G. K., Carns, T. K., Rhee, S. S., and Wang, K. L., "Selective Etching of SiGe on SiGe/Heterostructures", J. Electrochem. Soc. 138, 202 (1991).

Park, J. S., Karunasiri, R. P. G., Mii, Y. J., and Wang, K. L., "Hole Intersubband Absorption In δ-Doped Multiple Si Layers", Appl. Phys. Lett. 58, 1083, (1991).

Ma, Q. M., and Wang, K. L., "Strain-Induced Nonlinear Energy-Band Splitting of $Si_{1-x}Ge_x$ Alloys Coherently Grown on (111) and (110) Oriented Ge Substrates", Appl. Phys. Lett., 58 (11), 1184, (1991).

Karunasiri, R. P. G. and Wang K. L., "Quantum Devices Using SiGe/Si Heterostructures", J. Vac. Sci. Technol. B, 9, 2064, (1991).

Arbet-Engels, V., Kallel, M. A., and Wang, K. L., "Photoluminescence of Hydrogenated Si_mGe_n Superlattices", Appl. Phys. Lett. 59, 1705 (1991).

Karunasiri, R. P. G., Park, J. S., Wang K. L., "$Si_{1-x}Ge_x/Si$ Multiple Quantum Well Infrared Detector", Appl. Phys. Lett., 59, 2588 (1991).

Park, J. S., Karunasiri, R. P. G., Wang K. L., "Normal Incident Infrared Detector Using p-type SiGe/Si Multiple Quantum Wells", Appl. Phys. Lett.,61, 681 (1992).

Dafesh, P.A., and Wang K.L., "Temperature Dependences of the E_0 Transitions in Bulk Ge and a Ge-rich Si_mGe_n Superlattice", Phys. Rev. B, 45, 1712 (1991).

Karunasiri, R. P. G., Wang, K. L., and Park, J. S., "Intersubband Transitions in SiGe/Si Quantum Structures", Semiconductor Interfaces and Microstructures, World Scientific Publishing, pp 252-279 (1992)

Contributions to Conferences

Kallel, M. A., Arbet, V. P. Karunasiri, R. P. G., and Wang., K. L., "Characterization of Si_mGe_n Monolayer Using Photoluminescence", 10th MBE Conference, North Carolina State University, Sept. 13-15, 1989.

Park, J. S., Karunasiri, R. P. G., and Wang, K. L., "Observation of Large Stark Shift in Ge_xSi_{1-x}/Si Multiple Quantum Wells", 10th MBE Conference, North Carolina State University, Sept. 13-15, 1989.

Prokes, S. M., Fatemi, and Wang, K. L., "X-ray Study of Interdiffusion in Si/Ge Si Strained Layer Superlattice", 10th MBE Workshop, North Carolina State University, Sept. 13-15, 1989.

Wang, K. L., "Properties of Devices of SiGe Heterostructures and Superlattices", Int'l Conference on VLSI and CAD, Seoul, Korea, Oct. 17- 20, 1989.

Wang, K. L., "Band Engineering of Quantum Wells and Superlattices", National Chiao-Tung University, Oct. 21-23, 1989.

Rhee, S. S., Chang, G. K., Carns, T. K., and Wang, K. L., "Three Terminal SiGe Resonant Tunneling Transistor", 1989 IEEE-Int'l Electron Device Meeting, Washington, D. C., Dec. 3-6, 1989.

Arbet, V., Chang, S. J., and Wang, K. L., "PIN Photocurrent Studies of Monolayer Si_mGe_n Superlattices", SPIE 8th Technical Conference on Superlattice Physics Ultrafast Processes Nanostructures High Speed Electronics, San Diego, CA, Mar. 17-20, 1990.

Dafesh, P. A., Arbet, V. P., and Wang, K. L., "Electronic Transitions in a Ge Rich-Symmetrized Si_8Ge_{32} Superlattice Measured by Photoreflectance Spectroscopy", SPIE 8th Technical Conference on Superlattice Physics Ultrafast Processes Nanostructures High Speed Electronics, San Diego, CA, Mar. 17-20, 1990.

Wang, K. L., "Devices and Circuits Applications of SiGe Heterojunctions", 1990 IEEE-Int'l Symposium on Circuits and Systems (ISCAS), New Orleans, LO, May 1-3, 1990.

Wang, K. L., "Resonant Tunneling of Holes in Strained Layer Structures", NATO Workshop on Resonant Tunneling Physics and Applications, El Escorial, Spain, May 10-22, 1990.

Mii, Y. J., Karunasiri, R. P. G., Wang, K. L., and Yuh, P. F., "Large Stark Shift of Intersubband Transitions in Step Quantum Wells", 48th Device Research Conference, Santa Barbara, June 25-27, 1990.

Kallel, M. A., Wang., K. L., Karunasiri, R. P. G., and Arbet, V. P., "Optical Properties of Si_mGe_n Strained Monolayer Superlattices", 20th International Conference on the Physics of Semiconductors, Thessaloniki, Greece, Aug. 6-10, 1990.

Karunasiri, R. P. G. and Wang K. L., "Quantum Devices Using SiGe/Si Heterostructures", 37th National AVS Symposium and Topical Conferences, Toronto, Canada, Oct. 8-13, 1990.

Arghavani, M. R. and Wang K. L., "Angle Resolved X-ray Photoelectron Spectroscopy on Strained Ge_xSi_{1-x} Alloys", 37th National AVS Symposium and Topical Conferences, Toronto, Canada, Oct. 8- 13, 1990.

Kallel, M. A., Arbet-Engels, V., Wang, K. L., and Karunasiri, R. P. G., "MBE Si_mGe_n Strained Monolayer Superlattices", 6th International Conference on MBE, San Diego, CA, Aug. 27-31, 1990.

Wang, K. L., "Intersubband Transitions in Step Quantum Wells", Workshop on Optical Properties of Mesoscopic Semiconductor Structures, Snowbird, Utah, Apr. 23-26, 1991.

Kennedy, T. A, Glaser,E. R., Trombetta, J. M., Wang, K. L. and Chern, C. H., "Characterization of $Si_{1-x}Ge_x$/Si Heterostructures Using Optically-Detected Magnetic Resonance", the 4th International Symposium on Si Based MBE, Anaheim, California, Apr. 27-May 4, 1991.

Khorram, S., Chern, C. H., and Wang K. L., "Measurement of Valence Band Offset In Strained Ge_xSi_{1-x}/Si Heterojunctions", the 4th International Symposium on Si Based MBE, Anaheim, California, Apr. 27- May 4, 1991.

Park, J. S., Karunasiri. R. P. G., Wang K. L., Mii, Y.J., and Murray J., "Observation of Intersubband Absorption In Boron -Doped Si Layers", the 4th International Symposium on Si Based MBE, Anaheim, California, Apr. 27-May 4, 1991.

Karunasiri, R. P. G., Park, J. S., and K. L. Wang, "Long Wavelength (10 μm) Infrared Detector Using $Si_{1-x}Ge_x$/Si Multiple Quantum Wells", the 49th Annual Device Research Conference, Boulder, Colorado, June 17-19, 1991.

Dafesh, P. A., Arbet, V., and Wang k. L., "Characterization of the Interdiffusion Behavior in Si_mGe_n Superlattices Using Photoreflectance", the EMC Meeting in Boulder, Colorado, June 19-21, 1991.

Arbet-Engels, V., Karunasiri, R. P. G., Park, J. S., Lee, C., and Wang, K. L. "Effect of $HydroGe_n$ Passivation on Intersubband Absorption in Doped Si Layers", the EMC Meeting Boulder, Colorado, June 19-21, 1991.

Wang, K. L., Park, J. S., and Karunasiri R. P. G., "Intersubband Absorption In $Si_{1-x}Ge_x$/Si and -Doped Si Multiple Quantum Wells", the 5th International Conference on Modulated Semiconductor Structures, Nara, Japan, July 8-12, 1991.

Chern, C. H., Tijero, J. M. G., Wang, K. L., and S. J., Wang, " Resonant Magnetotunneling of Ge_xSi_{1-x} Resonant Tunneling Structures Grown At Extremely Low Temperature By MBE", 11th Annual MBE Workshop, The University of Texas, Austin, Texas, Sept. 16-18, 1991.

Lee, Chanho and Wang, K. L., "Intersubband Absorption in Sb d- doped MBE Si Quantum Well Structures", 11th MBE workshop, The University of Texas, Austin, Texas, Sept. 16-18, 1991.

Wang K. L., Arbet-Engels, V., Park, J. S., Kallel, M. A.,"$HydroGe_n$ation of SiGe/Si Layered Structures", Hydro Workshop, Freiburg, Germany, November 3-6, 1991
.

Arbet-Engels, V. P., Kallel, M. A., Wang, K. L., "$HydroGe_n$ Passivation of Defects-related Luminescence Signals in Si_mGe_n Superlattices", the APS March Meeting, Indianapolis, Indiana, March 16- 20, 1992.

Rusu, I. M., Karunasiri, R. P. G., and Wang, K. L., "Intersubband Absorption in -doped SiGe/Si Multiple Quantum Wells", the APS March Meeting, Indianapolis, Indiana, March 16-20, 1992.